Effects of valve timing, valve lift and exhaust backpressure on performance and gas exchanging of a two-stroke GDI engine with overhead valves

Macklini Dalla Nora*, Thompson Diórdinis Metzka Lanzanova, Hua Zhao

Centre for advanced powertrain and fuels (CAPF) – Brunel University London

Kingston Lane, Uxbridge, Middlesex UB8 3PH – United Kingdom

Corresponding author (*): Macklini.dallanora@brunel.ac.uk Phone: +44 (0)74630 95392

Highlights:

- Two-stroke operation was achieved in a four-valve direct injection gasoline engine;
- Shorter valve opening durations improved torque at lower engine speeds;
- The longer the valve opening duration, the lower was the air trapping efficiency;
- Higher exhaust backpressure and lower valve lift reduced the compressor work;

Keywords:

- Supercharged two-stroke cycle engine
- Overhead poppet valves
- Variable valve actuation
- Gasoline direct injection

Abstract

The current demand for fuel efficient and lightweight powertrains, particularly for application in downsized and hybrid electric vehicles, has renewed the interest in two-stroke engines. In this framework, an overhead four-valve spark-ignition gasoline engine was modified to run in the two-stroke cycle. The scavenging process took place during a long valve overlap period around bottom dead centre at each crankshaft revolution. Boosted intake air was externally supplied at a constant pressure and gasoline was directly injected into the cylinder after valve closure. Intake and exhaust valve timings and lifts were independently varied through an electrohydraulic valve train, so their effects on engine performance and gas exchanging were investigated at 800 rpm and

2000 rpm. Different exhaust backpressures were also evaluated by means of exhaust throttling. Air trapping efficiency, charging efficiency and scavenge ratio were calculated based on air and fuel flow rates, and exhaust oxygen concentration at fuel rich conditions. The results indicated that longer intake and exhaust valve opening durations increased the charge purity and hence torque at higher engine speeds. At lower speeds, although, shorter valve opening durations increased air trapping efficiency and reduced the estimated supercharger power consumption due to lower air short-circuiting. A strong correlation was found between torque and charging efficiency, while air trapping efficiency was more associated to exhaust valve opening duration. The application of exhaust backpressure, as well as lower intake/exhaust valve lifts, made it possible to increase air trapping efficiency at the expense of lower charging efficiency.

Abbreviations

AFR_{CYL}: in-cylinder air/fuel ratio, AFR_{EXH}: exhaust air/fuel ratio, ATDC: after top dead centre, BDC: bottom dead centre, BP: backpressure, CA: crank angle, CAI: controlled auto-ignition, CE: charging efficiency, C_P: specific heat of air at constant pressure, ECR: effective compression ratio, EER: effective expansion ratio, EVC: exhaust valve closing, EVL: exhaust valve lift, EVO: exhaust valve opening, IMEP: indicated mean effective pressure, IVC: intake valve closing, IVL: intake valve lift, IVO: intake valve opening, m_{TRAP}: in-cylinder trapped air mass, LHV: lower heating value, LVDT: linear variable displacement transducer, MBT: minimum spark advance for best torque, $\dot{m}$: air mass flow rate, P_{AMB}: ambient pressure, P_{INT}: intake pressure, RGF: residual gas fraction, SOI: start of injection, SR: scavenge ratio, T_{AMB}: ambient temperature, TE: air trapping efficiency, UHC:

unburned hydrocarbon, V_{CLR}: clearance volume, V_{CYL}: in-cylinder volume, $\dot{W}_C$: compressor power requirement, $[O_2]_{AMB}$: ambient oxygen concentration, $[O_2]_{EXH}$: exhaust oxygen concentration, λ_{CYL}: in-cylinder lambda, λ_{EXH}: exhaust lambda, ρ_{INT}: intake air density, γ: ratio of specific heats, η_C: compressor isentropic efficiency, η_i: indicated efficiency, η_M: compressor mechanical efficiency.

1. Introduction

The concept of engine downsizing has been adopted as the most feasible solution to four-stroke spark-ignition engines to attend upcoming CO_2 emission legislations. Following this principle the engine operation region is shifted towards higher loads by decreasing its swept volume and the number of cylinders. Therefore, large improvements in fuel consumption are obtained from lower pumping losses at higher intake pressures. To ensure the same full load performance of larger engines, supercharging and/or turbocharging is used to improve the charge density [1]. The increased engine load and hence higher in-cylinder temperature/pressure results in greater structural and thermal stresses. The occurrence of knocking combustion becomes also more often due to more severe compression of the end-gas [2], as well as higher probability of low-speed pre-ignition [3][4]. Conversely, two-stroke engines have the inherent advantage of doubled firing frequency compared to four-stroke engines, so the same output torque can be achieved with one half the indicated mean effective pressure (IMEP). The lower engine load, and consequently reduced structural robustness required, has made the two-stroke cycle mostly used for light weight vehicles. Its application as range extender in hybrid electric vehicles has been also evaluated for such primarily reason [5]. In small engines the use of intake and exhaust ports is rather attractive considering production costs and complexity compared to four-stroke units. This justifies the success of crank-case mixture scavenged two-stroke engines for motorcycles and handheld equipment [6]. On the other end of two-stroke engine application field are the low-speed uniflow-scavenged marine engines, with displacements in the order of cubic metres and brake efficiencies in excess of 50% [7][8][9].

The use of two-stroke engines in passenger cars, although, is constrained by three main factors: irregular combustion at low loads, fuel short-circuiting in mixture-scavenged engines and crank train durability issues [10]. At low loads two-stroke engines present large portions of burned gases trapped in the cylinder. Such dilution increases the heat capacity of the charge and reduces the oxygen availability resulting in unstable combustion and misfire [11]. When an efficient management of residual gas is performed through exhaust throttling [12][13] or overhead intake/exhaust valves [14][15][16], controlled auto-ignition (CAI) combustion can be achieved. This combustion mode improves combustion stability and fuel consumption by means of short burning durations and lower heat transfer [17].

Fuel short-circuiting is the main cause of unburned hydrocarbon (UHC) emissions in crankcase-mixture-scavenged two-stroke engines [18]. The use of direct fuel injection has addressed it at the cost of more complex and expensive fuel metering systems [19][20][21]. Despite such improvement, lubricant oil still needs to be added to the intake air to provide lubrication to the crank train components. To overcome this issue several concepts have been proposed, amongst which the uniflow-scavenged and the poppet-valve-scavenged are the most prominent. In such engines a conventional wet sump is employed similarly to that used in modern four-stroke engines. Two-stroke poppet valve engines have usually four overhead valves, which remain opened around bottom dead centre (BDC) every crankshaft revolution. Supercharger and/or turbocharger are responsible for supplying boosted intake air to scavenge the burned gases during the long valve overlap period. In the absence of ports, thermal distortion on piston and liner is avoided as the coolant jacket spreads uniformly around the cylinder [22]. Another advantage of poppet valve engines is the possibility of asymmetrical intake and exhaust valve operation [23]. In piston-controlled ported engines the gas exchanging is penalised at off-design conditions by the constant port timing, although the use of exhaust valves has partially addressed the issue [24].

Fuel short-circuiting in gasoline two-stroke engines with overhead valves can be readily avoided by direct fuel injection, although air short-circuiting from the intake to the exhaust system is still present. This is particularly found at high engine loads when great scavenging efficiencies are required to allow larger amounts of fuel to burn effectively. Several approaches have been investigated to reduce air short-circuiting, such as intake port deflector [25], masked cylinder head [20], stepped cylinder head [26], intake valve shrouding [27][28], and vertical intake ports [29].

The intake port deflector seen in Figure 1 (a) performs well at low engine loads, although at higher loads it largely restricts the intake air flow [25]. With a cylinder head mask, as shown in Figure 1 (b), air short-circuiting can be improved at all operating conditions despite the reduction in valve effective curtain area. This approach was recently used in a light duty two-cylinder Diesel engine [30]. The stepped cylinder head presents similar intake flow performance to the masked approach, even though the exhaust valve curtain region is also restricted as seen in Figure 1 (c). The use of shrouded valves seen in Figure 1 (d) improves the air trapping efficiency. However, methods to prevent the valves from spinning during the engine operation add complexity to this approach [27][28]. A wide range of valve shroud angles between 70° and 108° were found to perform well in a single cylinder four-valve 370 cm^3 engine [31]. Finally, the vertical intake port seen in Figure 1 (e) promotes the least flow restriction amongst all methods, although when solely used it cannot ensure high scavenging with low charge short-circuiting [26]. When employed in conjunction with a masked cylinder head, the vertical intake port improves the port's discharge coefficient [32]. Such configuration seen in Figure 1 (f) was employed in this research as it demonstrates a compromise between in-cylinder scavenging and flow restriction.

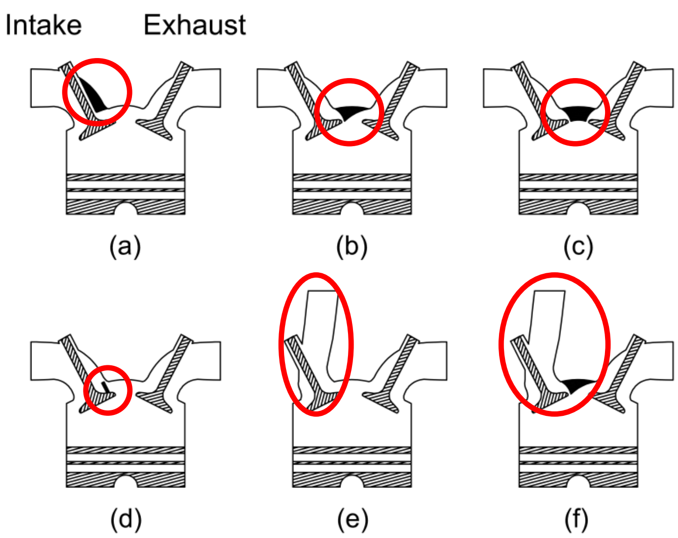

Figure 1 – Improvements in scavenging of two-stroke poppet valve engines: (a) intake port deflector, (b) masked cylinder head, (c) stepped cylinder head, (d) intake valve shrouding, (e) vertical intake port, and (f) masked cylinder head with vertical intake port.

The recent demand for high power density and low weight engines has renewed the interest in two-stroke poppet valve engines, particularly for application in diesel passenger cars [33][34] and hybrid electric vehicles [5][35]. Supercharged two-stroke engines with exhaust overhead valves have been also reported for use on general aviation and unmanned aerial vehicles [36]. Hence, with numerous improvements on variable valve actuation systems over the years [37][38], their application on the two-stroke cycle has the potential to greatly improve engine operation. Also, exhaust port restriction has been widely employed in ported two-stroke engines to improve torque and emissions over the years [39][40]. In poppet valve two stroke engines, although, its use has been mostly evaluated through numerical simulation to demonstrate the side effects of turbocharging [41][42]. In this framework, the present research experimentally investigates the effects of several intake/exhaust valve timings on gas exchanging and performance of a two-stroke GDI engine with overhead poppet valves. The effects of exhaust throttling in conjunction with low and full exhaust valve lift are also evaluated to explore the possible effects of turbocharging and/or aftertreatment systems. Meanwhile, intake valve lift was varied to evaluate the role played by the cylinder head mask on engine performance and gas exchange process.

2. Experiments

2.1 Experimental setup

The experiments were carried out in a Ricardo Hydra engine equipped with a fully variable electrohydraulic valve train unit, which provided independent control over intake and exhaust valves [43]. The 350 cm^3 engine displacement resulted from 81.6 mm bore and 66.9 mm stroke. The geometrical compression ratio was set to 11.8:1. Commercial UK gasoline (RON 95) was directly injected into the cylinder at 15.0±0.5 MPa and 293±5 K by a double-slit Denso injector side mounted between the intake ports. The fuel mass flow rate was measured by an Endress+Hauser Coriolis Promass 83A with a maximum error of ±0.2%. Spark timing, injection timing and duration, and valve events were managed by a Ricardo rCube unit, while the exhaust throttle was manually operated. A transient dynamometer enabled constant speed tests at 800 and 2000±5 rpm, while a LeineLinde incremental encoder with 720 pulses per revolution was employed to record the crank position. Intake and exhaust valve positions were recorded by four Lord DVRT linear variable displacement transducers (LVDT) with a resolution better than 6 μm and repeatability of ±1 μm. The signals from the LVDTs were pre-processed by a Lord Multichannel conditioner at 20 kHz, with a maximum error of 1% due to signal linearization. Valve opening and closing times were flagged at 0.7 mm of valve lift.

The boosted intake air necessary to scavenge the burned gases during the valve overlap was supplied by an AVL 515 compressor unit at a constant pressure of 135±4 kPa and temperature of 300±5 K. The air mass flow rate was measured by a Hasting HFM-200 laminar flow meter with a maximum error of 1%. Intake and exhaust pressures were acquired by two piezo-resistive transducers installed in the intake plenum (4007BA20F) and exhaust port (4007BA5F), with a maximum error of ±0.1% each. At the same points the average temperatures were measured by K-type thermocouples with ±1% accuracy. A Kistler 6061B piezo-electric transducer was used to monitor the in-cylinder pressure with maximum error of ±0.5%. Engine oil and coolant temperatures were kept at 353±3 K. The exhaust oxygen concentration was measured by a Horiba MEXA 7170DEGR using a paramagnetic sensor, with an error smaller than 2%. A National Instruments 6353 USB X card was used for data acquisition purposes. The location of the instruments can be found in Figure 2, as well as the temperature and pressure measurement points labelled as “T” and “P”, respectively.

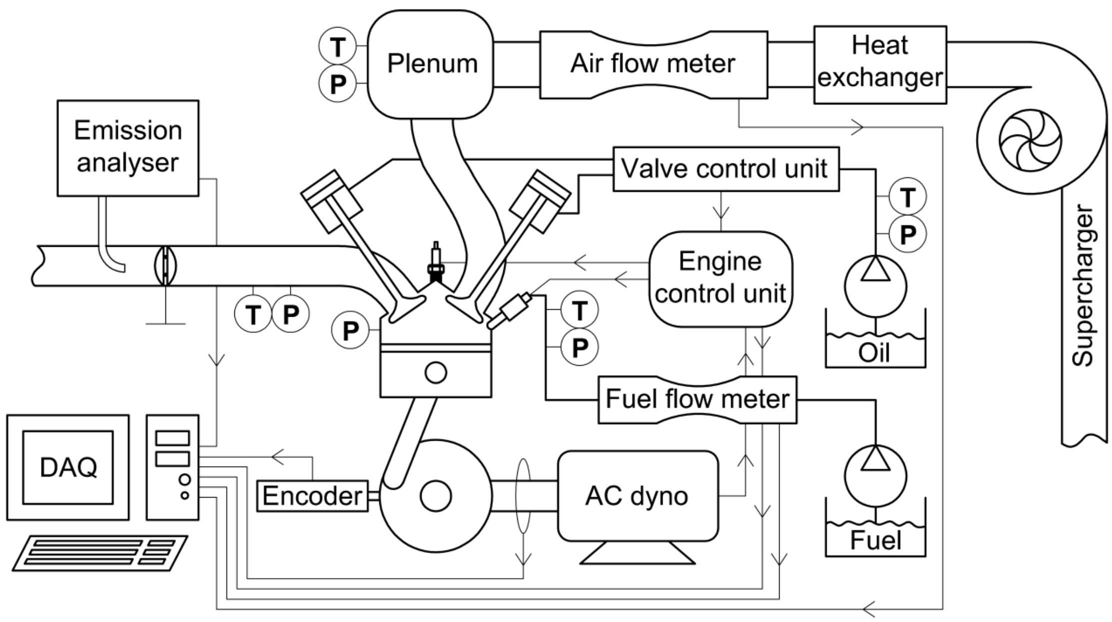

Figure 2 – Test cell facilities.

2.2 Data analysis

The air trapping efficiency (TE) is defined as the ratio of in-cylinder trapped air mass (m_{TRAP}) at intake or exhaust valve closing (whichever later) to the total air mass supplied every engine cycle (m_{TOT}). It was calculated based on the exhaust air/fuel ratio (AFR_{EXH}), exhaust oxygen concentration ($[O_2]_{EXH}$) and ambient oxygen concentration ($[O_2]_{AMB}$), considered 209500 ppm, as presented in Equation (1) from [44].

$$TE = \frac{m_{TRAP}}{m_{TOT}} = 1 - \frac{(1 + AFR_{EXH})[O_2]_{EXH}}{AFR_{EXH}[O_2]_{AMB}} \tag{1}$$

The in-cylinder lambda (λ_{CYL}) differed from the exhaust lambda (λ_{EXH}) as a result of air short-circuiting from the intake to the exhaust during the scavenging process. In all tests λ_{EXH} was found greater than λ_{CYL} and always above the unit, which is normally used in four-stroke engines for aftertreatment purposes. The exhaust lambda, calculated from air and fuel flow rate measurements, was multiplied by the air trapping efficiency so the in-cylinder lambda could be obtained as presented in Equation (2).

$$\lambda_{CYL} = \frac{AFR_{CYL}}{AFR_{STOICH}} = \lambda_{EXH}\, TE = \frac{AFR_{EXH}}{AFR_{STOICH}} \left(1 - \frac{(1 + AFR_{EXH})[O_2]_{EXH}}{AFR_{EXH}[O_2]_{AMB}}\right) \tag{2}$$

To ensure a minimum amount of free oxygen in the exhaust, and therefore avoid under prediction of air trapping efficiency, the in-cylinder lambda was kept in the range 0.93 - 0.95 at all tests. The fuel-rich in-cylinder mixture was obtained by measuring and processing on real-time air and fuel flow rates alongside the exhaust oxygen concentration. This calculation method based on exhaust oxygen detection is known to provide excellent results under homogeneous air-fuel charging processes, such as through port fuel injection systems [6]. However, the use of direct fuel injection induced a certain level of fuel stratification and therefore some inaccuracies may have taken place during the measurements. Considering this, the start of injection (SOI) was set as early as possible to improve the charge homogeneity but respecting intake valve closing (IVC) and exhaust valve closing (EVC) to avoid fuel short-circuiting. Furthermore, the engine speeds tested i.e. 800 rpm and 2000 rpm were low in comparison to small/mid-sized two-stroke engines. This enabled a longer charge preparation, so better fuel vaporisation and mixing with air and residual gas could be obtained.

The scavenge ratio (SR) is defined as the ratio of total inlet air mass to the in-cylinder reference mass at intake conditions. This reference mass was calculated from the in-cylinder volume (V_{CYL}) at IVC or EVC, whichever later, and the intake air density (ρ_{INT}). The clearance volume (V_{CLR}) was also considered as seen in Equation (3) from [6].

$$SR = \frac{m_{TOT}}{(V_{CYL} + V_{CLR})\rho_{INT}} \tag{3}$$

The charging efficiency (CE) was used to quantify how efficiently the cylinder was filled with air. It expresses the ratio between in-cylinder trapped air mass at IVC or EVC (whichever later) and the in-cylinder reference mass at intake conditions. Therefore, it results from the product between scavenge ratio and air trapping efficiency as shown in Equation (4).

$$CE = \frac{m_{TRAP}}{(V_{CYL}+V_{CLR})\rho_{INT}} = SR * TE \quad \therefore \quad RGF \cong 1 - CE \tag{4}$$

Under idealized flow conditions i.e. the scavenging process occurring at isobaric and isothermal conditions, burned and unburned zones may assume identical densities [6]. Thus, the residual gas fraction (RGF) can be roughly estimated from the difference between the charging efficiency and the unit.

The effective expansion ratio (EER) was determined by the in-cylinder volume at exhaust valve opening (EVO) or intake valve opening (IVO), whichever earlier. Similarly, the effective compression ratio (ECR) was calculated at EVC or IVC, whichever later, as presented in Equation (5).

$$EER \text{ and } ECR = \frac{V_{CYL} + V_{CLR}}{V_{CLR}} \tag{5}$$

In real world conditions part of the output power of the two-stroke poppet valve engine would be delivered to an external air compressor. Therefore, this supercharger power requirement ($\dot{W}_C$) was estimated based on the first and second laws of thermodynamics in a total to static compression process shown in Equation (6) from [45].

$$\dot{W}_C = \dot{m} C_P T_{AMB} \left(\left(\frac{P_{INT}}{P_{AMB}} \right)^{\frac{\gamma - 1}{\gamma}} - 1 \right) \frac{1}{\eta_C \eta_M} \quad (6)$$

where $\dot{m}$ is the air mass flow rate, C_P is the specific heat of air at constant pressure (considered 1.004 kJ/kg.K), T_{AMB} is the ambient temperature, P_{INT} is the engine intake pressure, P_{AMB} is the ambient pressure, γ is the ratio of specific heats (considered 1.40), η_C is the compressor isentropic efficiency (considered 0.70), and η_M is the compressor mechanical efficiency (considered 0.85). It is known that these efficiencies, particularly the isentropic efficiency, largely change with pressure ratio and air flow rate. Nevertheless, these values were estimated based on contemporary mechanically driven radial flow compressors [46], which are generally more efficient than roots type superchargers.

Four-stroke engines have one firing cycle every two revolutions and hence their IMEP values are twice as high as those found in two-stroke engines of the same displacement and running at the same speed. Therefore, to avoid misunderstandings in the loads achieved in the two-stroke cycle, the indicated specific torque (T_{is}) was employed as seen in Equation (7).

$$T_{is} = \eta_i m_{TRAP} \left(\frac{LHV}{2\pi V_{CYL} AFR_{CYL}} \right) \quad (7)$$

where LHV is the lower heating value of the fuel and η_i is the indicated efficiency.

2.3 Evaluation of valve timings

Intake and exhaust valve operations were centred at 185° and 175° of crank angle (CA) after top dead centre (ATDC), respectively, based on previous experimental observation [47]. Valve opening durations were independently varied from 50° CA to 150° CA (intake) and from 70° CA to 170° CA (exhaust). An increment of 20° CA was used between each testing point as shown in Figure 3 and Figure 4 for intake and exhaust valves, respectively. While the exhaust valve opening duration was fixed at a constant value, the intake valve timing was varied. After this, the exhaust valve timing was varied 20° CA and another set of intake durations was evaluated. The procedure was repeated until the peak torque was achieved at 800 rpm and 2000 rpm at both intake and exhaust duration sweeps. The valve lifts were set to 8 mm in all cases. The nomenclature used from Figure 7 to Figure 13 consists of intake and exhaust valve opening and closing times, in this sequence. For instance, in the case "In 130/240, Ex 120/230" the intake valves opened at 130° CA ATDC and closed at 240° CA ATDC, while the exhaust valves opened at 120° CA ATDC and closed at 230° CA ATDC.

In total, 25 different valve timings were experimentally assessed. To avoid the interference of the air-fuel mixing process on the results, the SOI was set to 260° CA ATDC, which was the latest IVC/EVC timing studied. In this case no fuel short-circuiting, as well as its backflow to the intake port, were expected to happen so the fuel trapping efficiency could be maximised. Knocking combustion limited the spark timing advance in all cases at both engine speeds. In other words, the earliest ignition timing towards the minimum spark advance for best torque (MBT) was applied.

Figure 3 – Intake valve opening duration sweep.

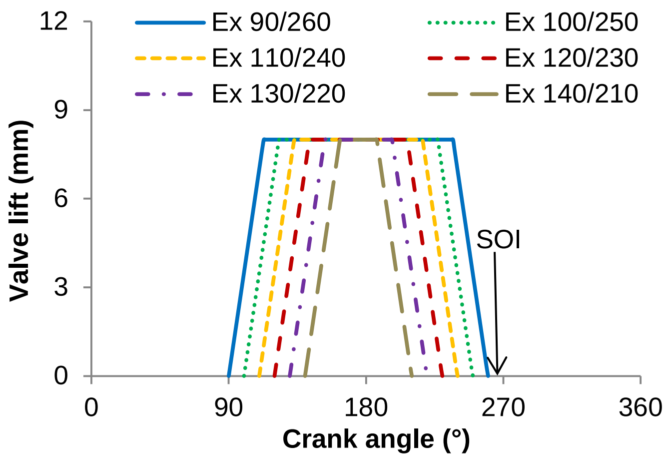

Figure 4 – Exhaust valve opening duration sweep.

2.4 Evaluation of valve lift and exhaust backpressure

Intake and exhaust valves were independently evaluated at 3 mm and 8 mm of lift as seen in Figure 5. The valve timing chosen in this case was that which presented appreciable output torque at 800 rpm and 2000 rpm, simultaneously, in the valve timing assessment. The 3 mm of valve lift matched the cylinder head mask height around the intake valves as shown in Figure 6. On the other hand, the 8 mm of lift represented the maximum value achieved by the electrohydraulic valve train unit and uncovered the head mask in 5 mm. It was also close to the dimensionless valve lift of 0.3 L/D (where “L” is the valve lift and “D” is the valve diameter). This is accepted as a limiting value beyond which the discharge coefficient presents small changes [45]. Therefore, the influence of the cylinder head mask on gas exchanging and engine performance could be investigated. The nomenclature used from Figure 14 to Figure 20 consists of intake valve lift (IVL) followed by exhaust valve lift (EVL), with the related numbers indicating the valve lifts in millimetres.

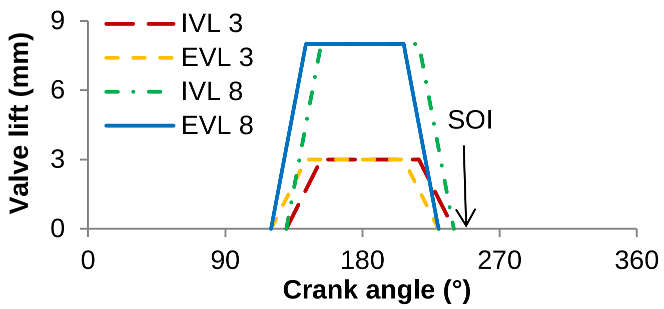

Figure 5 – Intake and exhaust valve lift sweeps.

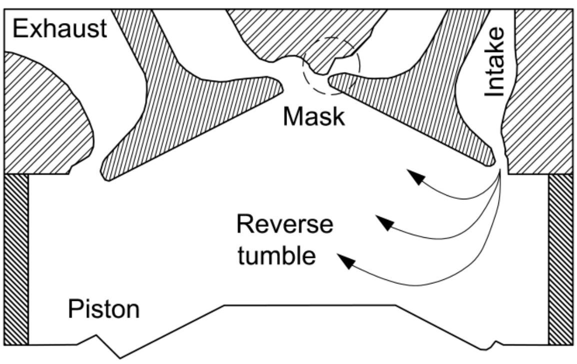

Figure 6 – Masked cylinder head and arrangement of intake/exhaust ports. Adapted from [47].

For each of the 12 different intake/exhaust valve lifts examined, three exhaust backpressures (BP) i.e. ~104 kPa, 110 kPa and 120 kPa were studied. The lowest exhaust backpressure tested was that of typical silencer and pipes, which remained between 103 kPa and 104 kPa depending on the valve lift used. For instance, the case “IVL 3, EVL 8, BP 110” used 3 mm and 8 mm of lift in the intake and exhaust valves, respectively, with an exhaust backpressure of 110 kPa. The SOI was advanced towards IVC (240° CA ATDC) to enhance the mixture homogeneity. In all cases the spark timing advance was limited by knocking combustion and MBT could not be achieved.

3. Results and discussion

The following results were averaged over 200 consecutive cycles and plotted as a function of valve timing, lift and exhaust backpressure at 800 rpm and 2000 rpm. In the valve opening duration plots (Figure 7 to Figure 13) the dashed lines represent the trend of the exhaust valve sweep. Each of the six plots in the figures represents an individual intake valve sweep at constant exhaust valve timings. The exhaust valve opening duration decreases from the left to the right in each figure, while the intake opening duration decreases from the left to the right in each plot. In the valve lift and exhaust backpressure results (Figure 14 to Figure 20), the dashed lines represent the exhaust backpressure sweeps increasing from the left to the right. Each of the three plots denotes the intake and exhaust valve lift sweeps at a constant exhaust backpressure.

3.1 Assessment of different valve timings

For all the 25 valve timings tested, the indicated specific torque was found in the range from 76 Nm/dm^3 to 185 Nm/dm^3. In values of IMEP this load spanned from 0.48 MPa to 1.16 MPa. This means that a four-stroke engine of the same swept volume would need to be operated from 0.96 MPa to 2.32 MPa to deliver the same torque at the same speed.

The indicated specific torque presented in Equation (7) is a function of indicated efficiency, charging and fuelling characteristics. Values between parentheses in that equation i.e. lower heating value of the fuel, exhaust air/fuel ratio and cylinder volume were kept constant during the tests. Meanwhile, the in-cylinder trapped air mass corresponded to the combination of air trapping efficiency and scavenge ratio, which is therefore the charging efficiency defined in Equation (4). Finally, the indicated efficiency was mostly a function of EER and ECR presented in Figure 8. The influence of combustion parameters i.e. combustion duration and phasing, were not independently considered as they were linked to ECR and scavenging process at the constant air/fuel ratio set.

At 800 rpm the specific torque increased at shorter intake/exhaust valve opening durations until “intake valve sweep 5”, as seen from the left to the right side along the X-axis in Figure 7. This was a result of increasing EER and ECR at more retarded EVO/IVO and more advanced EVC/IVC, respectively. At extremely short valve durations, although, EER and ECR effects were offset by the shorter time available for scavenging and a large amount of residual gas was trapped. The greater RGF caused the in-cylinder charge temperature to increase and more retarded spark timings were used to avoid knocking combustion, therefore reducing the output torque. The inflexion point was found around 90° CA of intake/exhaust valve duration (In 140/230, Ex 130/220). Therefore, other than this operating point the engine torque deteriorated with either longer or shorter valve opening durations. In contrast, at 2000 rpm longer exhaust durations were made necessary to allow an effective scavenging process, as the time available to it was reduced. Besides the greater frictional flow losses at 2000 rpm, the scavenging process also suffered from the smaller effective flow area resulted from the actuation speed of the electrohydraulic valve train. The valve opening and closing durations were constant on a time basis and not on a crank angle basis as in conventional engines. Therefore, the higher the engine speed the less steep the opening/closing slopes became, which reduced the effective flow area. Excessively long exhaust valve opening durations also decreased the specific torque as seen in intake valve sweeps 1 and 2 (first and second plots in Figure 7). The lower ECR and EER (Figure 8) reduced the specific torque in these cases. The torque could be only partially recovered by higher charging efficiencies at longer intake valve opening durations (e.g. “In 110/260, Ex 90/260” and “In 120/250, Ex 100/250”) as seen in Figure 9.

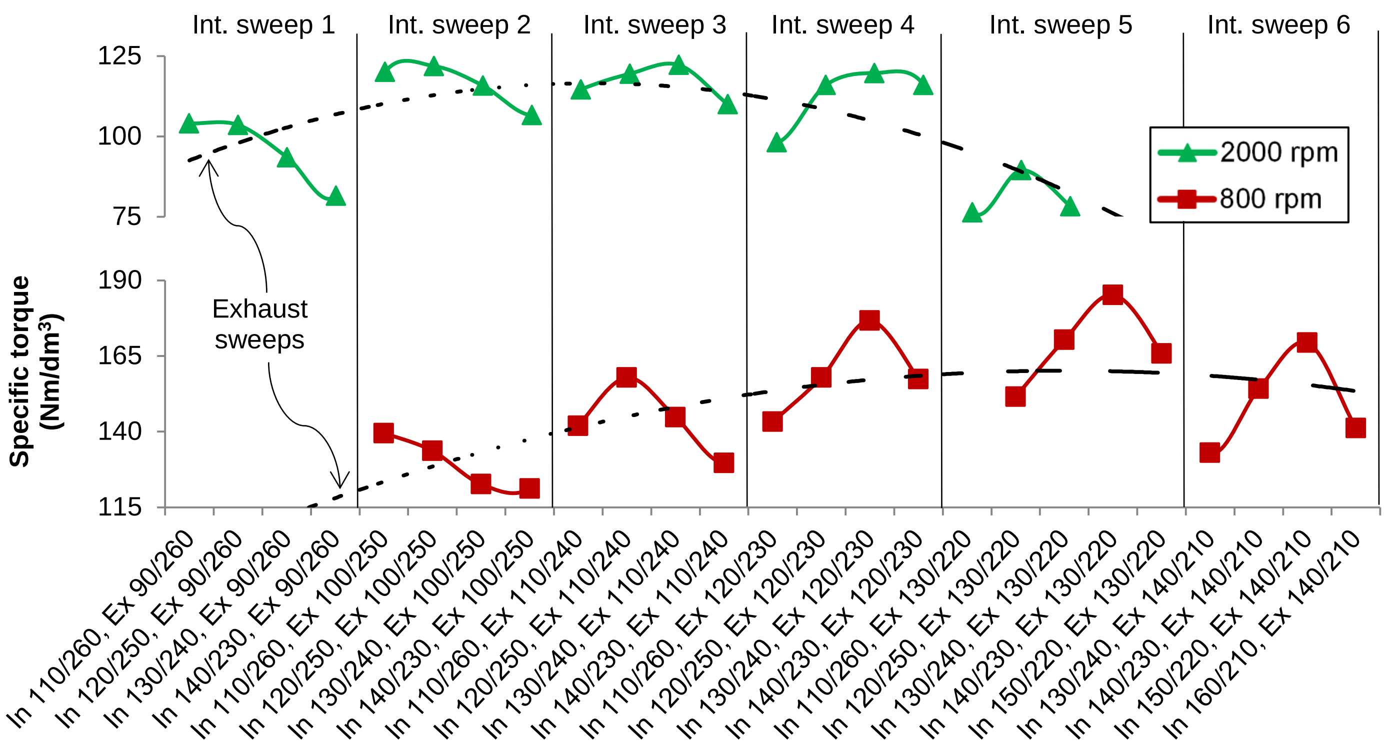

Figure 7 – Indicated specific torque results for the valve timing sweep.

As exhaust valve opening was retarded towards BDC, the EER increased and a higher torque was expected. However, as the in-cylinder pressure decreased close to BDC, the pressure ratio across the exhaust valves also dropped at EVO and the scavenging process was hindered by the weak exhaust blowdown. The highest specific torque of 185 Nm/dm^3 was achieved at 800 rpm with the valve timing “In 140/230, Ex 130/220”. At 2000 rpm the maximum torque of 122 Nm/dm^3 was reached with “In 130/240, Ex 110/240”. At lower speeds the longer time available for gas exchange enabled earlier EVC and hence a reasonable ECR of 10.3:1. Meanwhile, at 2000 rpm the time available for scavenging deteriorated and EVC was delayed, which reduced the ECR to about 8.8:1. This reduction in ECR is not desirable and the higher the speed the poppet valve engine is to achieve, the lower it will be due to the increased valve opening duration required. For the sake of comparison, mid/high-speed ported two-stroke engines typically operate with a constant ECR of about 6 to 7:1 [22].

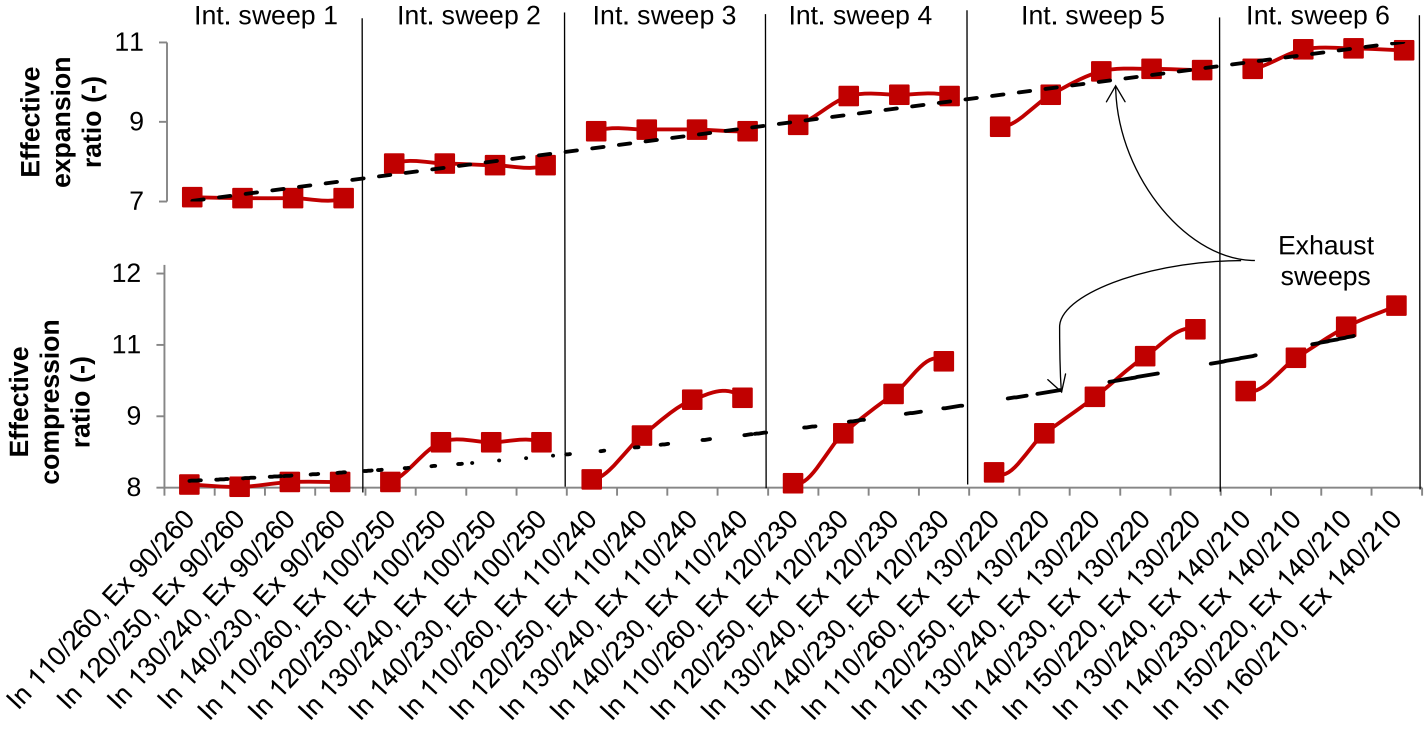

Figure 8 – Effective expansion and compression ratio results for the valve timing sweep.

The specific torque (Figure 7) and charging efficiency (Figure 9) results suggested that the shorter the exhaust duration, the shorter should be the intake duration as well. This effect was observed by the moving "peak" in the curves at both engine speeds tested, although at 800 rpm it was more pronounced. At 800 rpm and in the second intake valve sweep, the peak torque was near the first point investigated of "In 110/260, Ex 100/250". As the exhaust valve duration decreased, the peak torque moved towards shorter intake durations as seen in the third intake valve sweep in the case "In 120/250, Ex 110/240". Between these two cases the exhaust duration was shortened by 20° CA, while the intake duration was reduced by the same amount to produce the maximum torque. The common characteristic amongst all peak torque points found at 800 rpm was that EVO took place 10° CA before IVO. This ensured an effective exhaust blowdown phase before intake valve opening. When the intake valve opened before this 10° CA limit, intake backflow occurred and the charge purity decreased. Conversely, when IVO took place long after EVO the exhaust blowdown weakened and the pressure ratio across the exhaust valves dropped excessively until the scavenging process could start.

Another common feature amongst the highest torque points at 800 rpm was that IVC took place 10° CA after EVC. This configuration increased the charging efficiency (Figure 9) by providing a “supercharging effect” at the onset of compression [22]. In other words, at EVC the in-cylinder pressure was somewhat above exhaust pressure but below inlet pressure due to the valves restriction (in the absence of wave tuning). Therefore, by closing the intake valves after the exhaust valves more time was allowed for the in-cylinder pressure to increase towards the intake pressure, which was always higher than the exhaust pressure (in average). Some degree of ram effect was also expected to increase the charging efficiency based on the inertia of the intake air. Furthermore, the earlier EVC avoided the fresh charge from exiting the cylinder through the exhaust valves at such low speed. In conventional two-stroke engines, where the symmetric port arrangement makes it prohibitive to close the intake port(s) after the exhaust port(s), some of the fresh charge leaves the cylinder during the scavenging process. This shortcoming is often improved by exhaust timing valves at low engine speeds [40] and by wave propagation in tuned exhaust pipes [6] at high engine speeds. Nevertheless, when IVC took place long after EVC backflow occurred as the in-cylinder pressure became higher than the inlet pressure at IVC. The case “In 110/260, Ex 110/240” was such an example where the backflow reduced charging efficiency and consequently the output torque. At 2000 rpm the peak charging efficiency and torque were obtained when both IVC and EVC occurred at the same time, which indicated the need for longer intake/exhaust valve opening durations at higher engine speeds to improve the scavenging. At engine speeds above 2000 rpm one would expect the peak torque to occur at an EVC beyond IVC, which is the case of conventional ported two-stroke engines.

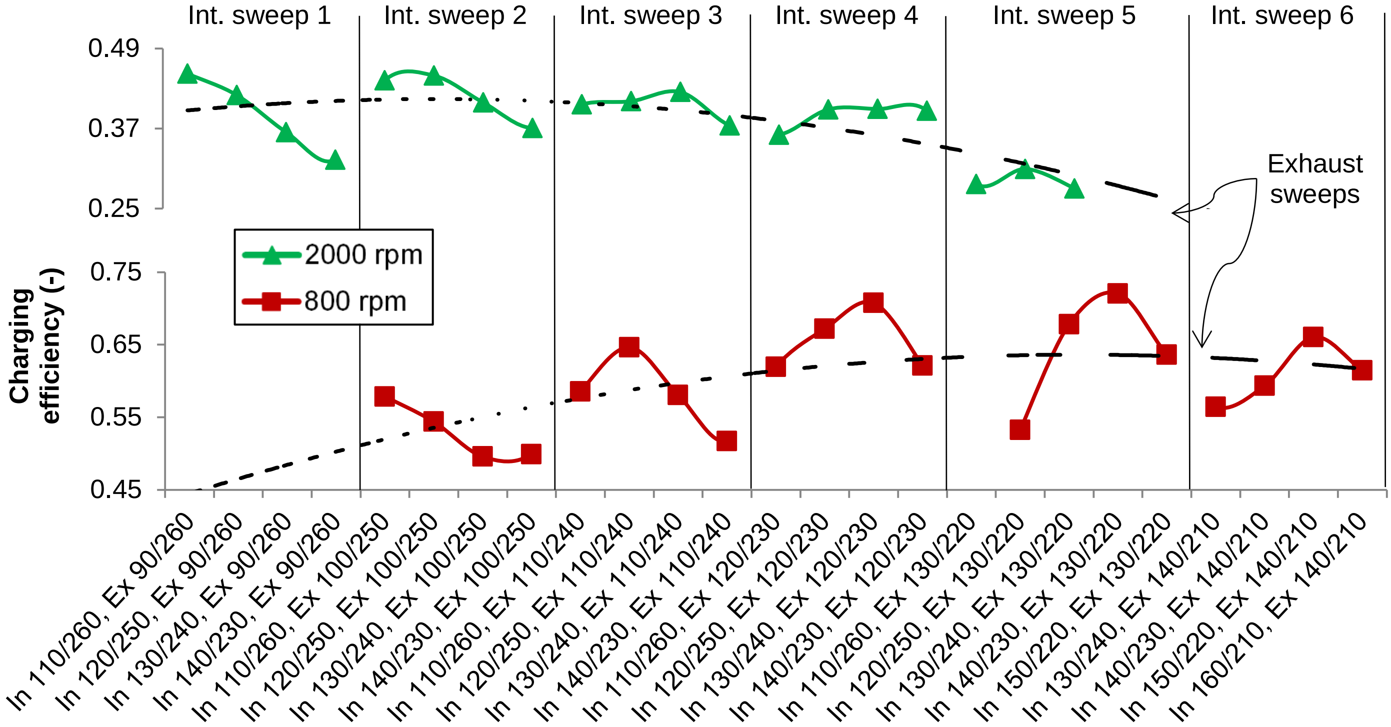

Figure 9 – Charging efficiency results for the valve timing sweep.

From Figure 7 and Figure 9 it is evident the strong correlation between charging efficiency and output torque as also reported in the literature [48]. An interesting event seen in Figure 9 was the reduction in charging efficiency when intake and exhaust valves opened at the same time as in the cases “In 120/250, Ex 120/230” and “In 130/240, Ex 130/220”. Both cases preceded the highest charging efficiencies points at 800 rpm and the reduction in torque by opening all the valves at the same time was around 10%. In these cases not only the effectiveness of the blowdown was reduced but a higher in-cylinder pressure at IVO also hindered the initial phase of the scavenging process. At 2000 rpm the difference in charging efficiency between the highest torque cases and those when intake/exhaust valves were opened at the same time decreased to about 4%. This behaviour suggested that the exhaust blowdown phase was not very critical in the scavenging process at higher speeds under lower values of scavenge ratio as observed in Figure 10. Furthermore, the first portion of air entering the cylinder is usually mixed with burned gases and expelled in the exhaust [22]. Thus, the air contamination in the intake ports when IVO and EVO took place together had little effect on the purity of the trapped charge, as the cylinder was actually filled with a later portion of the inducted air at the onset of compression.

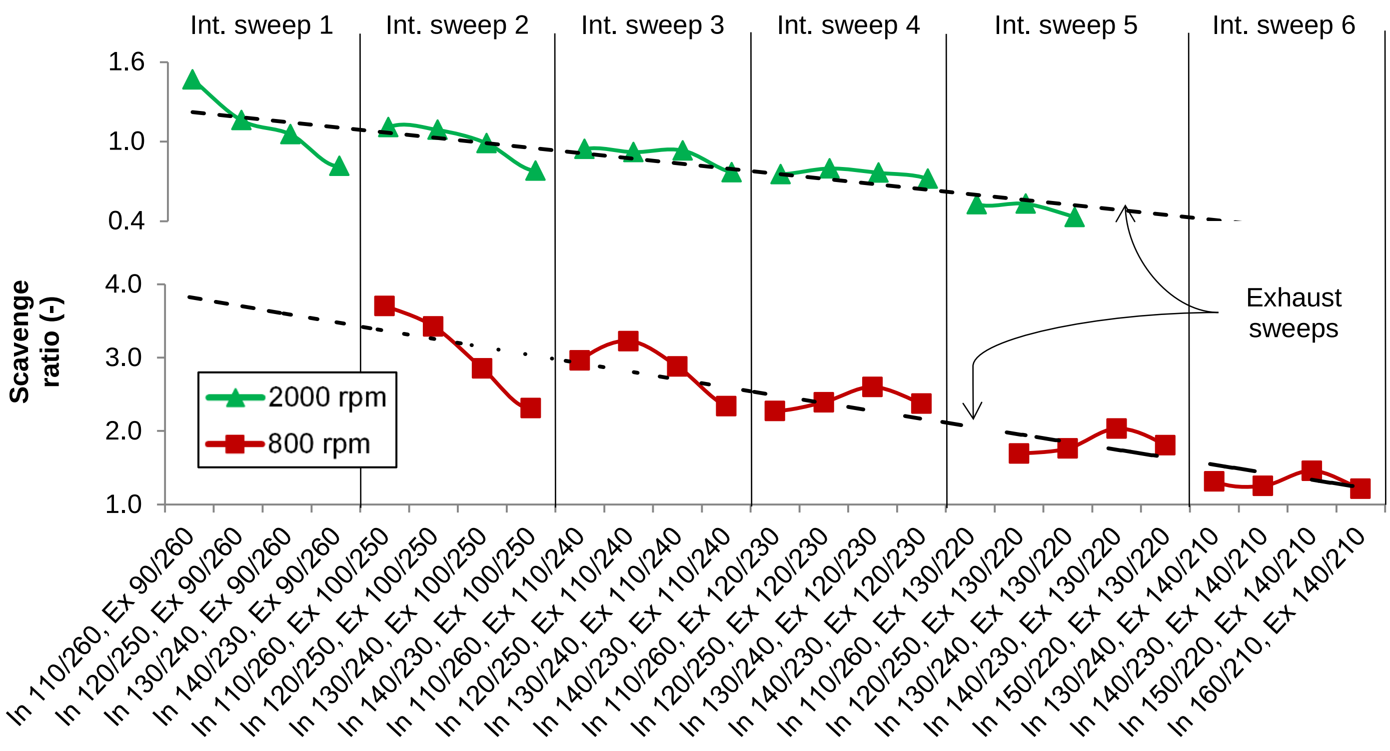

Figure 10 – Scavenge ratio results for the valve timing sweep.

The scavenge ratio seen in Figure 10 increased linearly with exhaust valve opening duration. At 2000 rpm the engine operation was not possible at intake/exhaust valve opening durations below 110°/90° CA, respectively, as a result of scavenge ratios as low as 0.43 and air trapping efficiencies of up to 0.65. The large RGF in these cases elevated the in-cylinder charge temperature and required the spark timing to be retarded to avoid knocking combustion. The exceedingly retarded values of ignition timing resulted in unstable combustion and misfire, so these operating points were disregarded.

From the exhaust sweep at 2000 rpm it was clear that even with intake and exhaust durations as long as 150° CA and 170° CA, respectively, the charging efficiency (Figure 9) could not increase above 0.45. The same impossibility of improving the charging process was found at 800 rpm as the intake and exhaust valve durations increased beyond 110° CA. At both speeds there was plenty of air supply as seen by the high scavenge ratio values in Figure 10. For the sake of comparison, at 800 rpm the scavenge ratio reached an overall maximum of 3.71, while in ported two-stroke engines this value rarely overtakes 1.5 at full load [6]. Under these circumstances the excess of air supplied was not efficiently scavenging the burned gases. Instead, it was actually being lost to the exhaust system. This fact was confirmed by the low values of air trapping efficiency found for these valve opening durations, particularly at 800 rpm. Figure 11 presents the clear correlation between air trapping efficiency and exhaust valve sweeps at both engine speeds, although at 2000 rpm it was more evident. Comparatively, the intake valve sweeps had a less pronounced effect on air trapping efficiency.

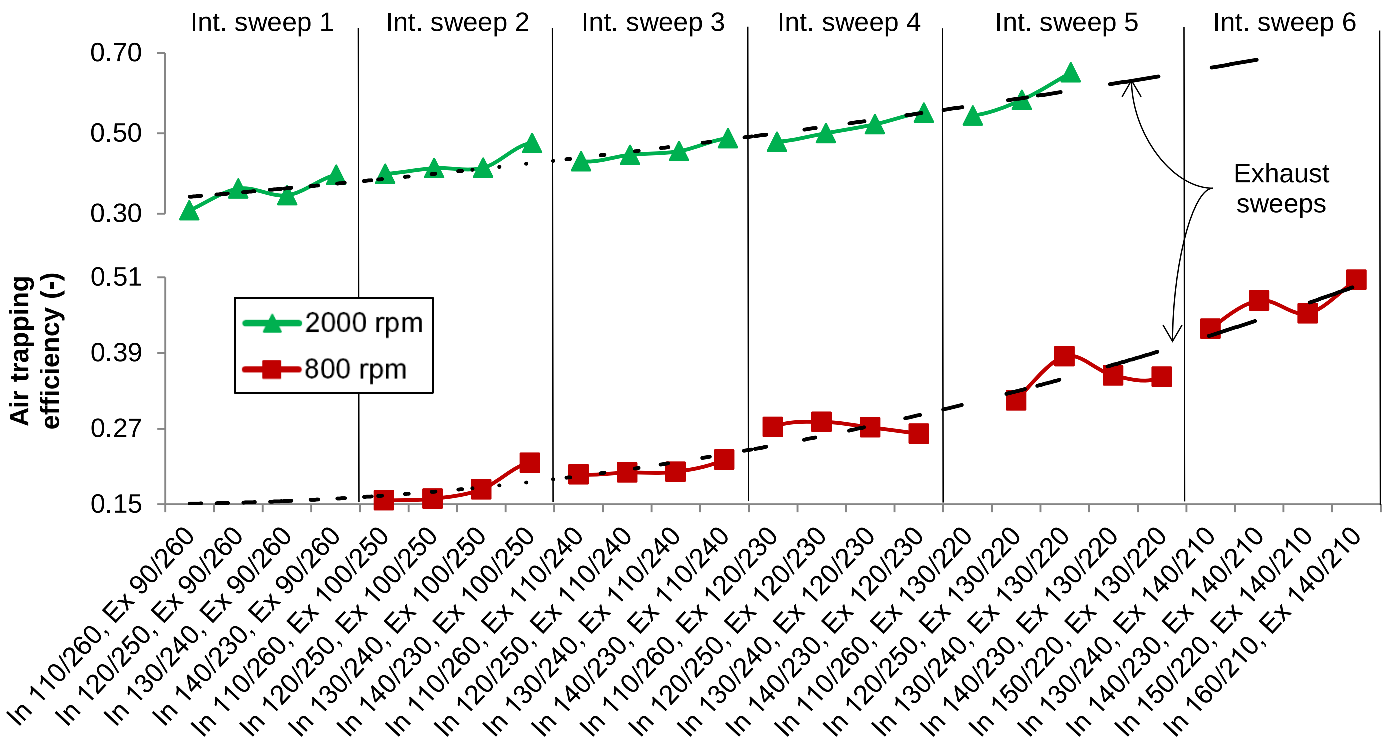

Figure 11 – Air trapping efficiency results for the valve timing sweep.

It is important to clarify that not all of the air present in the exhaust resulted from air short-circuiting, as assessed via air trapping efficiency calculation at fuel-rich in-cylinder conditions. Part of the intake charge mixed with the burned gases during the mixing-scavenging process, so it was not possible to distinguish the portions of short-circuited air from those mixed during the scavenging. The mixing-scavenging is still a form of scavenging, although it is not as efficient as perfect displacement. It is still better than pure short-circuiting, when the burned gas is not displaced from the combustion chamber.

Although the output torque was directly linked to the charging efficiency, high values of air trapping efficiency were also desirable to ensure that the fresh charge was not lost in the exhaust. As seen in Equation (4), charging efficiency is the product of air trapping efficiency and scavenge ratio. Thus, a higher output torque could not be achieved by only increasing the scavenge ratio at low values of trapped air mass. This was the case of very long exhaust valve durations, so the power consumed by the supercharger was considerably large as shown by its ratio to the indicated power in Figure 12.

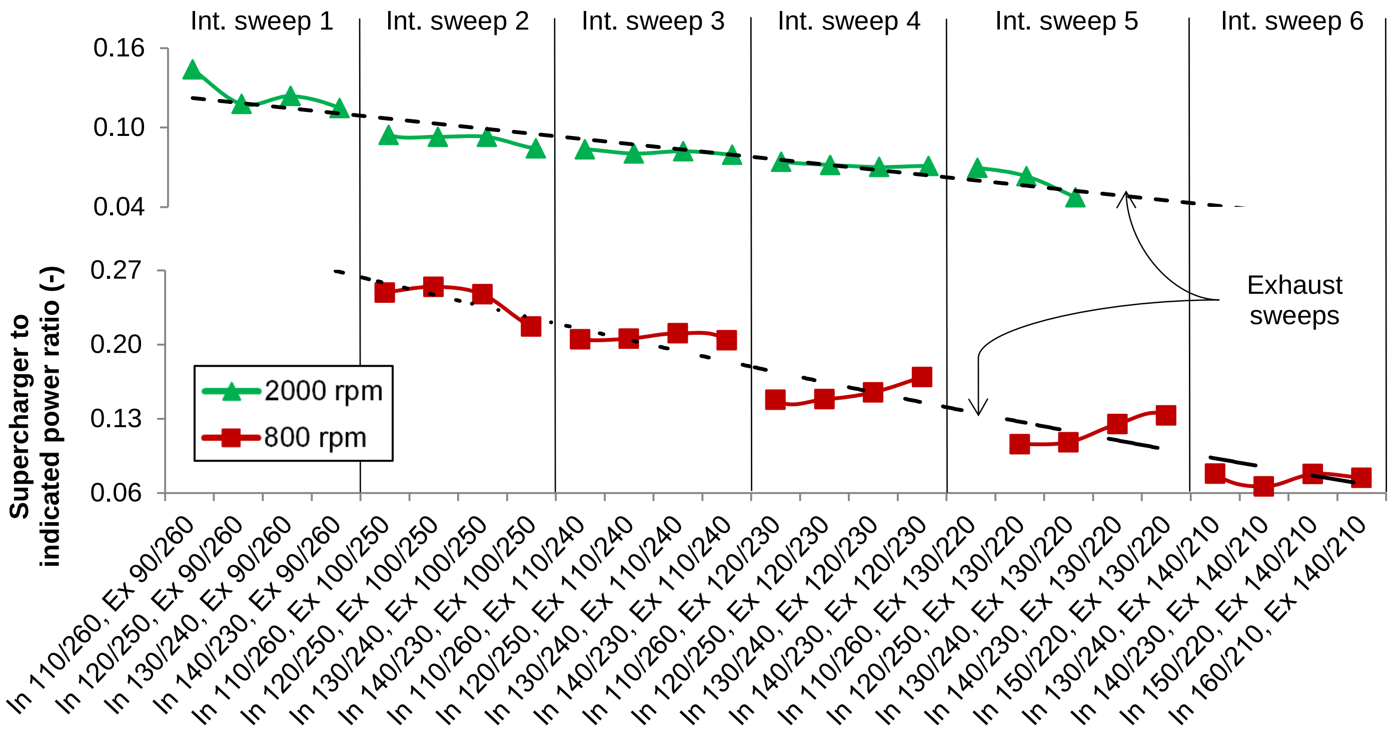

Figure 12 – Ratio of supercharger power requirement to engine indicated power for the valve timing sweep.

As the exhaust valve opening duration increased (right to left in plots), the air trapping efficiency dropped and a larger fraction of supplied air was lost in the exhaust. This waste of energy, particularly visible at 800 rpm, explained the greater values of supercharger power consumption on the left end intake sweeps (Figure 12). At both engine speeds the trend for this power ratio was considerably similar to the exhaust sweeps, while intake valve timing played again a less important role. Due to the lower scavenge ratio, higher air trapping efficiency, and greater indicated power at 2000 rpm, the fraction of power consumed by the supercharger remained between 5% and 14%. At 800 rpm the supercharger to indicated power ratio varied from 7% to 25%. Figure 13 reveals the best intake/exhaust valve timings to produce the highest possible net power, which was calculated by the subtraction of supercharger power consumption from the indicated power.

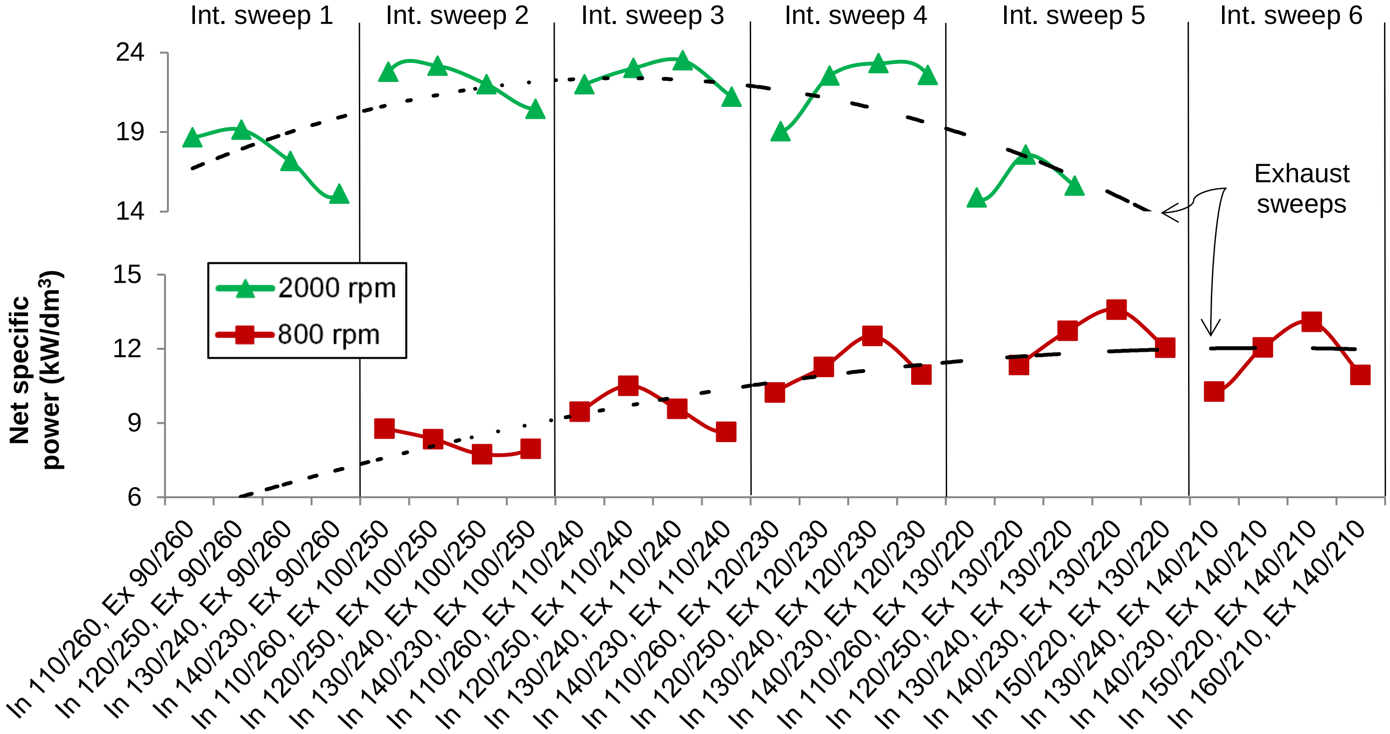

Figure 13 – Net indicated specific power considering the supercharger power consumption for the valve timing sweep.

At 800 rpm the valve timing “In 140/230, Ex 130/220” made it possible to achieve 13.6 kW/dm^3. The cases “In 150/220, Ex 140/210” and “In 130/240, Ex 120/230” reached 4% and 8% less power, respectively. At 2000 rpm nearly the same net specific power was obtained at the three “peaks” in intake sweeps 2, 3 and 4. A value of 23.3 KW/dm^3 (±2%) was acquired at “In 120/250, Ex 100/250”, “In 130/240, Ex 110/240” and “In 130/240, Ex 120/230”. This result demonstrated a certain flexibility of the engine for different valve configurations at higher speeds.

Aiming at a single valve timing to be tested with different valve lifts and exhaust backpressures, the case “In 130/240, Ex 120/230” was chosen for its reasonable performance at both speeds. At 800 rpm this case represented a reduction of about 8% in the net specific power compared to the best case, although at 2000 rpm the difference was irrelevant.

3.2 Assessment of different valve lifts and exhaust backpressures

From Figure 14 it is noticeable that any reduction of intake and exhaust valve lifts from the maximum value of 8 mm resulted in poorer torque at both speeds and any exhaust backpressure. The results suggested that the intake mask affected more the scavenging process than the flow restriction resulted from lower exhaust valve lift. While the masked region around the intake valves was supposed to increase air trapping efficiency through lower air short-circuiting, the decrease in charging efficiency was more pronounced (Figure 15) and hence the torque deteriorated. This fact was further evidenced by the gain in specific torque and charging efficiency when comparing the three last cases in the first lift sweep (Lift sweep 1). When IVL was increased from 3 mm to 8 mm and EVL reduced from 8 mm to 3 mm, the output torque increased by 20% at 2000 rpm. However, when EVL was raised from 3 mm to 8 mm at a constant IVL of 8 mm, the improvement in torque was around 4%. It is known that the scavenging process in ported two-stroke engines is strongly dependent on the exhaust port details. For the same reason, the two-stroke poppet valve engine used in this research has exhaust valves larger than intake valves (30 mm against 28 mm). However, there was no performance gain by fully opening the exhaust valves if the intake flow was restricted at 3 mm of valve lift as in the cases "IVL 3, EVL 8".

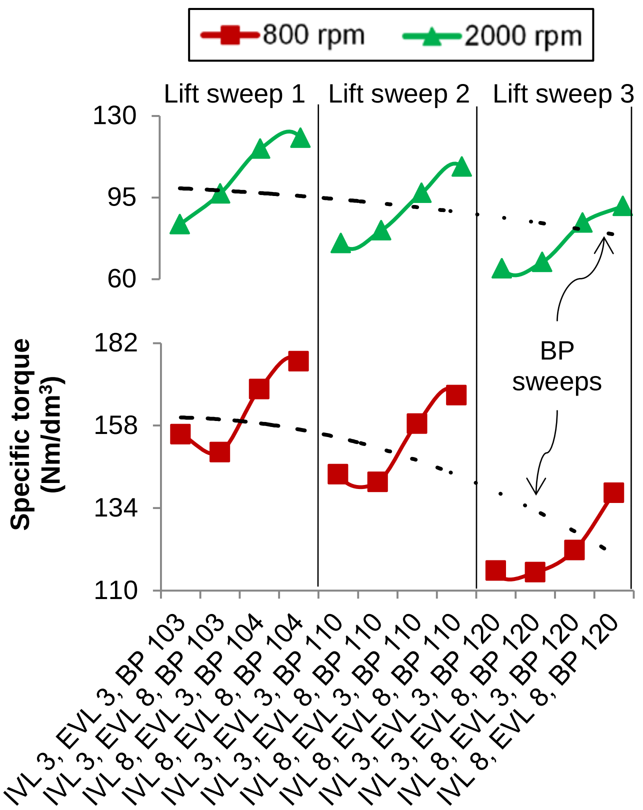

Figure 14 – Indicated specific torque results for the valve lift and exhaust backpressure sweeps.

The indicated specific torque trend at 800 rpm was not as linear as that at 2000 rpm because the cases with 3 mm of IVL and 8 mm of EVL presented poorer performance than those with 3 mm of IVL and EVL. This fact only happened at 800 rpm and was attributed to lower in-cylinder trapped air mass at the onset of compression. Despite the fact that IVC occurred after EVC in all cases, the greater exhaust valve area at 8 mm of lift allowed more fresh charge to leave the cylinder at such low speed. The low IVL imposed a greater restriction to the intake air flow and the incoming charge could not compensate for the lack of filling in only 10° CA between EVC and IVC. On the other hand, in the cases with IVL and EVL of 3 mm a larger in-cylinder trapped air mass was obtained thanks to the greater restriction imposed by the lower EVL. As the exhaust backpressure increased, more charge was trapped and the difference between 3 mm and 8 mm of EVL (at a constant IVL of 3 mm) vanished as supposed.

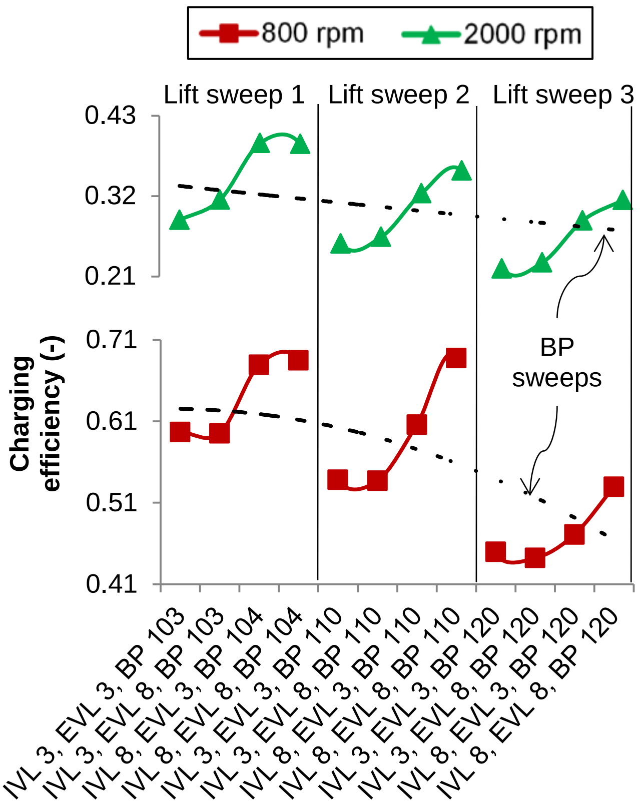

Figure 15 – Charging efficiency results for the valve lift and exhaust backpressure sweeps.

As the exhaust backpressure increased (from the left to the right in the plots), the output torque gradually deteriorated at both engine speeds. The increase in exhaust backpressure also hindered the effect of lower valve lifts at both speeds due to the reduction in pressure ratio across the valves. This was evidenced by the less steep curves in the specific torque and charging efficiency plots in Figure 14 and Figure 15, respectively. As previously discussed, the charging efficiency followed very closely the output torque profile. However, a distinct behaviour was found for the case “IVL 8, EVL 8, BP 110”. At 800 rpm this case provided similar values of charging efficiency than the last two cases in “Lift sweep 1” where no exhaust backpressure was applied. It indicated that a moderate exhaust backpressure of 110 kPa with full valve lift (IVL 8, EVL 8, BP 110) resulted in similar charging efficiency of the valve configuration for best torque (IVL 8, EVL 8, BP 104). Equivalent results were obtained at 3 mm of exhaust valve lift and no exhaust backpressure (IVL 8, EVL 3, BP 104). At 2000 rpm any exhaust throttling resulted in lower charging efficiency, although similar results of charging efficiency were again obtained with 3 mm or 8 mm of exhaust valve lift without backpressure. These results indicated that the exhaust was more efficient than the intake during the scavenging process, so the exhaust valves were oversized (or the intake valves were undersized) for the range of speeds evaluated. The poorer intake performance was a result of smaller inlet valves and the masked region around them.

Overall, charging efficiency was less affected by exhaust backpressure at 2000 rpm than at 800 rpm as seen by the dashed lines in Figure 15. Therefore, the exhaust backpressure offered by a turbocharger at higher engine speeds would not necessarily hinder the charging process, so part of the exhaust gas energy could be recovered. Results presented by [42] for a two-stroke poppet valve diesel engine suggested the use of a large turbocharger for scavenging the burned gases at high engine speeds only. Meanwhile, the low speed charging was ensured by a crankshaft driven supercharger. This configuration guaranteed minimum exhaust backpressure at low speeds but a moderate value at higher engine speeds.

While charging efficiency remained similar in the last two cases of “Lift sweep 1” and in the last case of “Lift sweep 2”, lower torque was observed at any valve lift or exhaust backpressure other than the optimum case of “IVL 8, EVL 8, BP 104”. This mismatch between torque and charging efficiency was attributed to higher in-cylinder temperatures resulted from more residual gas trapped at poorer exhaust flow (either because of lower lift or backpressure). In this case the spark timing was retarded to avoid knocking combustion and hence a lower torque was obtained. In Figure 16 it is observed that a higher scavenge ratio was found for the case “IVL 8, EVL 8, BP 104”. This meant that even at the same value of charging efficiency a larger portion of fresh air mass was delivered to the engine and reduced the charge temperature. The spark timing in this case was assessed and it was found that the ignition timing was advanced by 2° CA at 800 rpm and 4° CA at 2000 rpm towards MBT. At a constant value of charging efficiency and by increasing the scavenge ratio, the air trapping efficiency was expected to drop according to Equation (4). This was the situation as seen in Figure 17, once it dropped by 11% due to the use of 8 mm of EVL.

At both engine speeds the scavenge ratio dropped as the exhaust backpressure increased. This was obvious considering that the lower intake-exhaust pressure ratio drove less fresh air through the engine. The same trend was observed for the reduction in IVL and EVL as the valve effective flow area dropped. The reduction in scavenge ratio had a positive impact on air trapping efficiency at both speeds as seen in Figure 17. This was particularly the case when IVL was reduced from 8 mm to 3 mm and/or exhaust backpressure was set to its maximum value of 120 kPa. At 2000 rpm, 8 mm of IVL/EVL, and an exhaust backpressure of 110 kPa, the air trapping efficiency increased by 17% compared to the natural exhaust backpressure offered by the pipes and silencer.

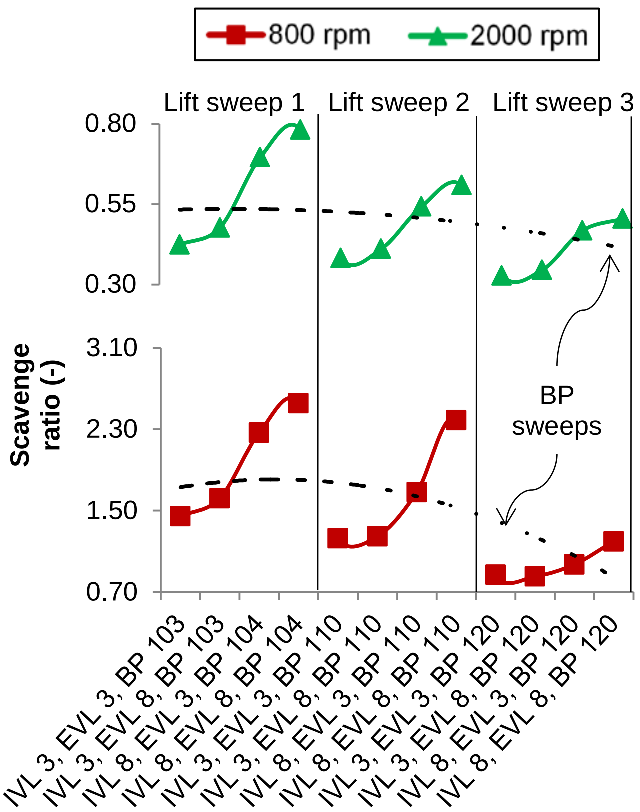

Figure 16 – Scavenge ratio results for the valve lift and exhaust backpressure sweeps.

At 8 mm of IVL the mask capacity of maintaining high values of air trapping efficiency deteriorated. For instance, at 2000 rpm it dropped by 17% when the intake valve lift increased from 3 mm to 8 mm as shown in the plot “Lift sweep 1” in Figure 17. Air trapping efficiency dropped further 12% when EVL increased from 3 mm to 8 mm as a result of increased valve effective flow area. There was also a peculiarity that reduced the air trapping efficiency when all valves were operated at maximum lift as seen in the last quadrant of Figure 18. Due to the increased pent-roof angle of the combustion chamber (126°), necessary to accommodate the four valves, fuel injector, and spark plug, there was a short path defined between intake and exhaust valves at full lift. This region enhanced the air short-circuiting and decreased air trapping efficiency. It could be observed that the exhaust backpressure raised by 1 kPa as the IVL increased from 3 mm to 8 mm (lift sweep 1), which justified this effect. Meanwhile, 3 mm of IVL minimised the air short-circuiting regardless the EVL employed. When 3 mm of lift was used for IVL and EVL (first quadrant in Figure 18), there were fewer paths for air short-circuiting to occur.

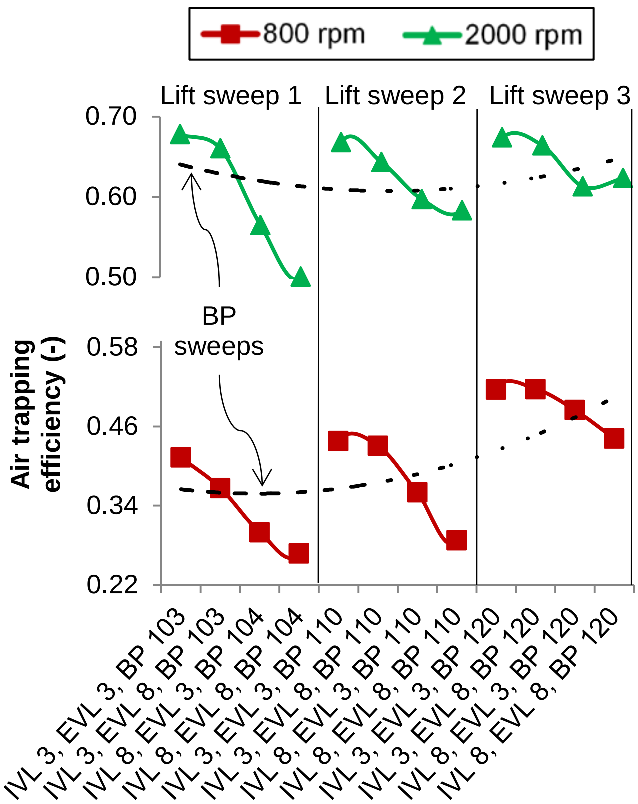

Figure 17 – Air trapping efficiency results for the valve lift and exhaust backpressure sweeps.

It is interesting to note the steep rise in supercharger power consumption (Figure 19) as the exhaust valve lift was increased from 3 mm to 8 mm at 800 rpm. Such increase was caused by the short air path seen in Figure 18, even though its effect was attenuated at higher exhaust backpressures. At 2000 rpm the most perceptible difference in supercharger power consumption took place as the IVL increased from 3 mm to 8 mm regardless the EVL used. This resulted from air trapping efficiency losses as the intake valves uncovered the masked region.

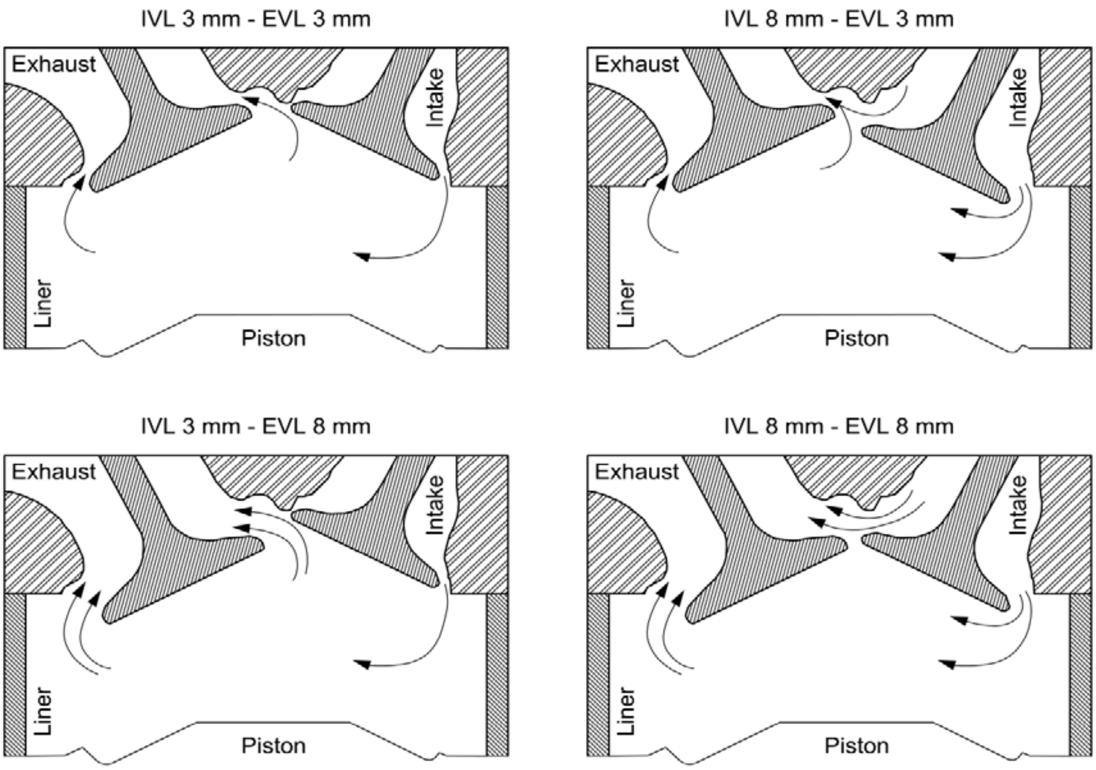

Figure 18 – Schematic representation of in-cylinder flow pattern at different valve lifts.

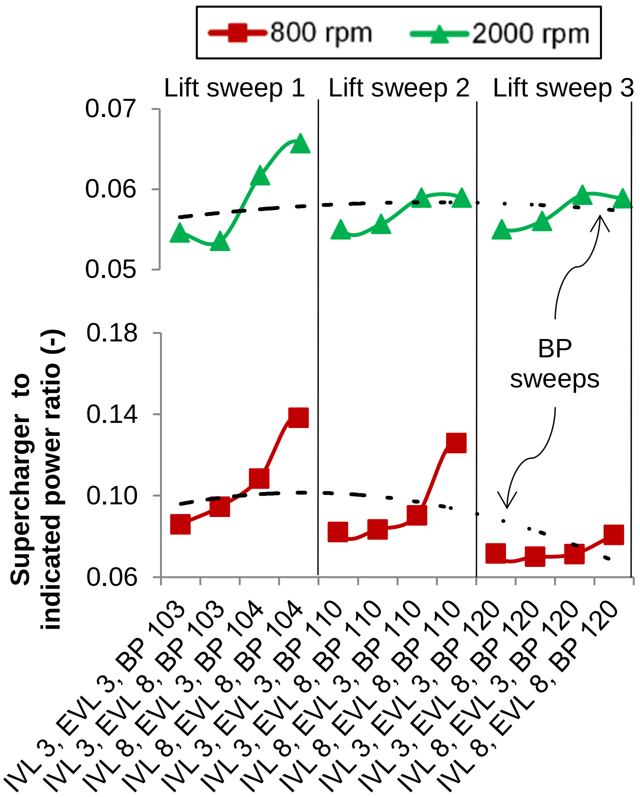

Figure 19 – Ratio of supercharger power requirement to engine indicated power for the valve lift and exhaust backpressure sweeps.

The net indicated specific power, presented in Figure 20, was calculated by subtracting the supercharger power consumption from the indicated power. At both engine speeds the maximum net power was achieved with no exhaust backpressure and full valve lift (IVL 8, EVL 8, BP 104). However, the difference in net power to the case with 3 mm of EVL (IVL 8, EVL 3, BP 104) remained low at both engine speeds. Therefore, a reduced EVL could increase air trapping efficiency without significantly deteriorating the output power. At 800 rpm this difference in net power was found below 2%, while at 2000 rpm it increased to about 3%. In addition, at 800 rpm an exhaust backpressure of 110 kPa could be applied with 8 mm of IVL/EVL without excessively compromising the output power compared to “IVL 8, EVL 8, BP 104”. In this scenario the net specific power reduced by about 4%, while air trapping efficiency improved by 8%. The reduction in exhaust dilution is favourable for aftertreatment systems as the exhaust gas temperature enhances and its oxygen content decreases. This fact impacts not only on the conversion efficiency of catalysts but also on the energy available in case of turbocharging.

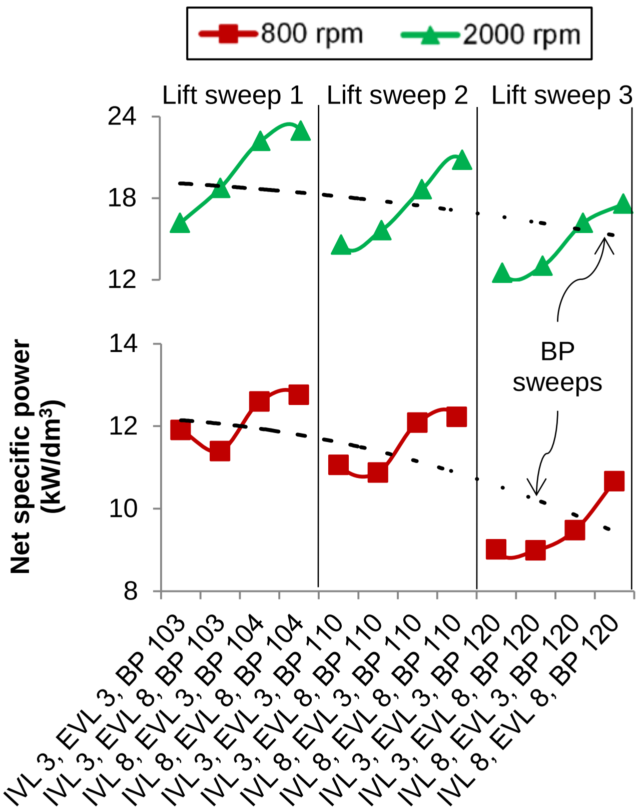

Figure 20 – Net indicated specific power results for the valve lift and exhaust backpressure sweeps.

Data presented in Figure 20 should be interpreted with caution, once the backpressure resulted from the application of a turbocharger would provide boosted intake air. Thus, it would enhance the net specific power of the cases on the right end of Figure 20 depending on the synergy and efficiency of the boosting system (supercharger + turbocharger).

4. Conclusions

Performance and gas exchanging of a two-stroke GDI engine with overhead poppet valves were evaluated at different valve timings, valve lifts and exhaust backpressures. Lower engine speeds benefited from shorter intake/exhaust valve opening durations. Meanwhile, at higher speeds the time available for gas exchange shortened and longer valve opening durations were required. Very long intake/exhaust opening durations, although, deteriorated the effective compression/expansion ratios and air trapping efficiency. Thus, the indicated power reduced and the supercharger power consumption increased at higher air short-circuiting rates. Similarly, excessively short valve opening durations resulted in poor charging efficiency and large amounts of residual gas trapped, requiring more retarded spark timings to avoid knocking combustion. Despite the improvements in EER and ECR, this condition resulted in deteriorated torque particularly at 2000 rpm. In all tests it was found a strong correlation between torque and charging efficiency, while air trapping efficiency was associated to exhaust valve opening duration.

With IVO at 130°, IVC at 240°, EVO at 120° and EVC at 230° CA ATDC, the engine performance was found satisfactory at both speeds tested. The 10° CA between EVO and IVO enabled an effective exhaust blowdown phase to take place without intake backflow. The 10° CA between EVC and IVC improved the charge purity at the onset of compression by means of a “supercharging effect”. This valve configuration was further evaluated regarding different intake and exhaust valve lifts and the effect of exhaust backpressure.

Any combination of intake and exhaust valve lifts, apart from 8 mm, resulted in torque deterioration at both speeds. At low intake valve lifts there were modest gains by opening the exhaust valves beyond the same values of lift. In addition, air trapping efficiency and supercharger power consumption were greatly improved by limited valve openings. Overall, the higher the exhaust backpressure, the lower was the output torque at both engine speeds. Nevertheless, the charging efficiency was less affected by the exhaust backpressure at higher engine speeds. At 800 rpm the air trapping efficiency could be improved by either lower exhaust valve lift or modest exhaust backpressure without compromising net power.

Acknowledgements

The first and second authors would like to acknowledge the Brazilian council for scientific and technological development (CNPq – Brasil) for supporting their PhD studies at Brunel University London.

References

[1] Martin S, Beidl C, Mueller R. Responsiveness of a 30 Bar BMEP 3-Cylinder Engine: Opportunities and Limits of Turbocharged Downsizing. SAE Tech. Pap., 2014. doi:10.4271/2014-01-1646.

[2] Zaccardi J-M, Pagot A, Vangraefschepe F, Dognin C, Mokhtari S. Optimal Design for a Highly Downsized Gasoline Engine. SAE Tech. Pap., 2009. doi:10.4271/2009-01-1794.

[3] Kalghatgi GT, Bradley D. Pre-ignition and “super-knock” in turbo-charged spark-ignition engines. Int J Engine Res 2012;13:399–414. doi:10.1177/1468087411431890.

[4] Wang Z, Qi Y, He X, Wang J, Shuai S, Law CK. Analysis of pre-ignition to super-knock: Hotspot-induced deflagration to detonation. Fuel 2015;144:222–7. doi:10.1016/j.fuel.2014.12.061.

[5] Mattarelli E, Rinaldini CA, Cantore G, Agostinelli E. Comparison between 2 and 4-Stroke Engines for a 30 kW Range Extender. SAE Int J Altern Powertrains 2014;4:2014–32 – 0114. doi:10.4271/2014-32-0114.

[6] Blair GP. Design and simulation of two-stroke engines. Warrendale: Society of Automotive Engineers; 1996.

[7] Haider S, Schnipper T, Obeidat A, Meyer KE, Okulov VL, Mayer S, et al. PIV study of the effect of piston position on the in-cylinder swirling flow during the scavenging process in large two-stroke marine diesel engines. J Mar Sci Technol 2013;18:133–43.

doi:10.1007/s00773-012-0192-z.

[8] Sigurdsson E, Ingvorsen KM, Jensen MV, Mayer S, Matlok S, Walther JH. Numerical analysis of the scavenge flow and convective heat transfer in large two-stroke marine diesel engines. Appl Energy 2014;123:37–46. doi:10.1016/j.apenergy.2014.02.036.

[9] Raptotasios SI, Sakellaridis NF, Papagiannakis RG, Hountalas DT. Application of a multi-zone combustion model to investigate the NOx reduction potential of two-stroke marine diesel engines using EGR. Appl Energy 2015;157:814–23. doi:10.1016/j.apenergy.2014.12.041.

[10] Kenny RG. Developments in two-stroke cycle engine exhaust emissions. Arch Proc Inst Mech Eng Part D J Automob Eng 1989-1996 (Vols 203-210) 1992;206:93–106. doi:10.1243/PIME_PROC_1992_206_165_02.

[11] Dalla Nora M, Lanzanova T, Zhang Y, Zhao H. Engine Downsizing through Two-Stroke Operation in a Four-Valve GDI Engine. SAE Tech. Pap., 2016. doi:10.4271/2016-01-0674.

[12] Asai M, Kurosaki T, Okada K. Analysis on Fuel Economy Improvement and Exhaust Emission Reduction in a Two-Stroke Engine by Using an Exhaust Valve. SAE Tech. Pap., 1995. doi:10.4271/951764.

[13] Andwari AM, Aziz AA, Said MFM, Latiff ZA. Experimental investigation of the influence of internal and external EGR on the combustion characteristics of a controlled auto-ignition two-stroke cycle engine. Appl Energy 2014;134:1–10. doi:10.1016/j.apenergy.2014.08.006.

[14] Zhang Y, Zhao H, Ojapah M, Cairns A. CAI combustion of gasoline and its mixture with ethanol in a 2-stroke poppet valve DI gasoline engine. Fuel 2013;109:661–8. doi:10.1016/j.fuel.2013.03.002.

[15] Zhang Y, Zhao H. Investigation of combustion, performance and emission characteristics of 2-stroke and 4-stroke spark ignition and CAI/HCCI operations in a DI gasoline. Appl Energy 2014;130:244–55. doi:10.1016/j.apenergy.2014.05.036.

[16] Benajes J, Martín J, Novella R, Thein K. Understanding the performance of the multiple injection gasoline partially premixed combustion concept implemented in a 2-Stroke high speed direct injection compression ignition engine. Appl Energy 2016;161:465–75.

doi:10.1016/j.apenergy.2015.10.034.

[17] Zhao H, editor. HCCI and CAI engines for the automotive industry. Cambridge: Woodhead Publishing; 2007.

[18] Hooper PR, Al-Shemmeri T, Goodwin MJ. Advanced modern low-emission two-stroke cycle engines. Proc Inst Mech Eng Part D J Automob Eng 2011;225:1531–43. doi:10.1177/0954407011408649.

[19] Shawcross D, Pumphrey C, Arnall D. A Five-Million Kilometre, 100-Vehicle Fleet Trial, of an Air-Assist Direct Fuel Injected, Automotive 2-Stroke Engine. SAE Int. J. Fuels Lubr., 2000. doi:10.4271/2000-01-0898.

[20] Nomura K, Nakamura N. Development of a new two-stroke engine with poppet-valves: Toyota S-2 engine. In: Duret P, editor. A new Gener. two-stroke enignes Futur., Paris: Technip; 1993, p. 53–62.

[21] Pradeep V, Bakshi S, Ramesh A. Direct injection of gaseous LPG in a two-stroke SI engine for improved performance. Appl Therm Eng 2015;89:738–47. doi:10.1016/j.applthermaleng.2015.06.049.

[22] Heywood JB, Sher E. The two-stroke cycle engine: its development, operation and design. Warrendale: SAE International–Taylor and Franci; 1999.

[23] Lu Y, Pei P, Liu Y. An evaluation of a 2/4-stroke switchable secondary expansion internal combustion engine. Appl Therm Eng 2014;73:323–32. doi:10.1016/j.applthermaleng.2014.07.075.

[24] Zhang S, Zhao Z, Zhao C, Zhang F, Wang S. Development and validation of electro-hydraulic camless free-piston engine. Appl Therm Eng 2016;102:1197–205. doi:10.1016/j.applthermaleng.2016.03.093.

[25] Nakano M, Sato K, Ukawa H. A Two-Stroke Cycle Gasoline Engine with Poppet Valves on the Cylinder Head. SAE Tech. Pap., 1990. doi:10.4271/901664.

[26] Tribotte P, Ravet F, Dugue V, Obernesser P, Quechon N, Benajes J, et al. Two Strokes Diesel Engine - Promising Solution to Reduce CO2 Emissions. Procedia - Soc Behav Sci 2012;48:2295–314. doi:10.1016/j.sbspro.2012.06.1202.

[27] Ukawa H, Nakano M, Sato K. A Two-Stroke Cycle Engine with Poppet Valves in the Cylinder Head - Part III: An Application of Gaseous Fuel Direct Injection System. SAE Tech. Pap., 1993. doi:10.4271/930983.

[28] Sato K, Ukawa H, Nakano M. A Two-Stroke Cycle Gasoline Engine with Poppet Valves in the Cylinder Head - Part II. SAE Tech. Pap., 1992. doi:10.4271/920780.

[29] Hundleby GE. Development of a Poppet-Valved Two-Stroke Engine - The Flagship Concept. SAE Tech. Pap., 1990. doi:10.4271/900802.

[30] Benajes J, Molina S, Novella R, De Lima D. Implementation of the Partially Premixed Combustion concept in a 2-stroke HSDI diesel engine fueled with gasoline. Appl Energy 2014;122:94–111. doi:10.1016/j.apenergy.2014.02.013.

[31] Yang X, Okajima A, Takamoto Y, Obokata T. Numerical Study of Scavenging Flow in Poppet-Valved Two-Stroke Engines. SAE Tech. Pap., 1999. doi:10.4271/1999-01-1250.

[32] Li Z, He B, Zhao H. The Influence of Intake Port and Pent-Roof Structures on Reversed Tumble Generation of a Poppet-Valved Two-Stroke Gasoline Engine. SAE Tech. Pap., 2014. doi:10.4271/2014-01-1130.

[33] Benajes J, Novella R, De Lima D, Tribotté P, Quechon N, Obernesser P, et al. Analysis of the combustion process, pollutant emissions and efficiency of an innovative 2-stroke HSDI engine designed for automotive applications. Appl Therm Eng 2013;58:181–93. doi:10.1016/j.applthermaleng.2013.03.050.

[34] Liu Y, Zhang F, Zhao Z, Dong Y, Ma F, Zhang S. Study on the Synthetic Scavenging Model Validation Method of Opposed-Piston Two-Stroke Diesel Engine. Appl Therm Eng 2016. doi:10.1016/j.applthermaleng.2016.03.094.

[35] Jia B, Smallbone A, Zuo Z, Feng H, Roskilly AP. Design and simulation of a two- or four-stroke free-piston engine generator for range extender applications. Energy Convers Manag 2016;111:289–98. doi:10.1016/j.enconman.2015.12.063.

[36] Carlucci AP, Ficarella A, Laforgia D, Renna A. Supercharging system behavior for high altitude operation of an aircraft 2-stroke Diesel engine. Energy Convers Manag 2015;101:470–80. doi:10.1016/j.enconman.2015.06.009.

[37] Knop V, Mattioli L. An analysis of limits for part load efficiency improvement with VVA devices. Energy Convers Manag 2015;105:1006–16. doi:10.1016/j.enconman.2015.08.065.

[38] De Bellis V, Gimelli A, Muccillo M. Effects of Pre-Lift Intake Valve Strategies on the Performance of a DISI VVA Turbocharged Engine at Part and Full Load Operation. Energy Procedia 2015;81:874–82. doi:10.1016/j.egypro.2015.12.141.

[39] Sher E, Hacohen Y, Refael S, Harari R. Minimizing Short-Circuiting Losses in 2-S Engines by Throttling the Exhaust Pipe. SAE Tech. Pap., 1990. doi:10.4271/901665.

[40] Hsieh P, Horng R, Huang H, Peng Y, Wang J. Effects of Exhaust Charge Control Valve on Combustion and Emissions of Two-Stroke Cycle Direct-Injection S.I. Engine. SAE Tech. Pap., 1992. doi:10.4271/922311.

[41] Brynych P, Macek J, Tribotte P, De Paola G, Ternel C. System Optimization for a 2-Stroke Diesel Engine with a Turbo Super Configuration Supporting Fuel Economy Improvement of Next Generation Engines. SAE Tech. Pap., 2014. doi:10.4271/2014-32-0011.

[42] Pohorelsky L, Brynych P, Macek J, Vallaude P-Y, Ricaud J-C, Obernesser P, et al. Air System Conception for a Downsized Two-Stroke Diesel Engine. SAE Tech. Pap., 2012. doi:10.4271/2012-01-0831.

[43] Osborne RJ, Stokes J, Lake TH, Carden PJ, Mullineux JD, Helle-Lorentzen R, et al. Development of a Two-Stroke/Four-Stroke Switching Gasoline Engine - The 2/4SIGHT Concept. SAE Tech. Pap., 2005. doi:10.4271/2005-01-1137.

[44] Douglas R. AFR and Emissions Calculations for Two-Stroke Cycle Engines. SAE Tech. Pap., 1990. doi:10.4271/901599.

[45] Heywood JB. Internal combustion engine fundamentals. New York: McGraw-Hill; 1988.

[46] Rotrex. Rotrex C15 supercharger - Technical datasheet v5.0 n.d. http://www.rotrex.com/Home/Products/Fixed-Ratio-Superchargers (accessed March 10, 2015).

[47] Dalla Nora M, Zhao H. High load performance and combustion analysis of a four-valve direct injection gasoline engine running in the two-stroke cycle. Appl Energy 2015;159:117–31. doi:10.1016/j.apenergy.2015.08.122.

[48] Kee RJ, Blair GP, Douglas R. Comparison of Performance Characteristics of Loop and Cross Scavenged Two-Stroke Engines. SAE Tech. Pap., 1990. doi:10.4271/901666.